Complexes of electropositive metals with a hemilabile ether phosphine. Crystal structures of [$TiCl_4L$], [$FeL_2(O_3SCF_3)_2$] and [$Mo(CO)_3L_2$] [L = $PhCH_2P(CH_2CH_2OEt)_2$]

Steven J. Chadwell, Simon J. Coles, Peter G. Edwards * and Michael B. Hursthouse

Department of Chemistry, University of Wales, Cardiff, PO Box 912, Cardiff CF1 3TB, UK

New complexes containing some early transition metals with benzylbis(2-ethoxyethyl)phosphine (L) have been prepared. Reaction of this potentially hemilabile terdentate ligand with $TiCl_4$ afforded [$TiCl_4L$] **1**. The crystal structure shows the metal to have a distorted-octahedral geometry, where the ligand acts as a P,O-bonding chelate. Reaction of **1** with $AgBF_4$ and AgO_3SCF_3 afforded yellow oils which could not be fully characterised, but are tentatively assigned as [$TiCl_3L$][BF_4] and [$TiCl_3L$][O_3SCF_3] respectively. The reaction of [$Cr(MeCN)_3(CO)_3$] with L resulted in the formation of [$Cr(CO)_4L_2$] **2** in poor yield. This complex can be prepared in high yield by the reaction of [$Cr(MeCN)_2(CO)_4$] with L. The reaction of [$M(CO)_3(C_6H_3Me_3$-2,4,6)] (M = Mo or W) with L gave the complex *fac*-[$Mo(CO)_3L_2$] **3** and [$M(CO)_4L_2$] (M = Mo **4** or W **5**) depending upon reaction conditions. The crystal structure of **3** shows the metal to have a distorted-octahedral geometry, where one L bonds as a P,O chelate and the other as a P-donor. ^{31}P-{^1H} NMR spectroscopy indicates this complex to be fluxional in solution, where the two ligands readily interchange at high temperatures. The iron(II) complex [$FeL_2(O_3SCF_3)_2$] **6** was prepared by the reaction of L and $FeCl_2 \cdot 4H_2O$ with AgO_3SCF_3. Its crystal structure shows the metal to have a distorted-octahedral geometry with *trans* ligands (through phosphorus and oxygen) and *trans*-co-ordinating triflates.

There has been considerable interest in the use of so-called hemilabile[1] ligands in recent years. These have at least two different co-ordination centres, *e.g.* phosphorus and nitrogen,[2] enabling the formation of complexes with one donor of the ligand strongly bound to the metal whilst the other is more weakly bound. The latter can dissociate from the metal so that the ligand bonds in a monodentate mode, allowing the formation of a free co-ordination site which may be important in homogeneous catalysis.[3] Many studies have concentrated on the use of phosphorus/oxygen ligands, including ketophosphines,[4] phosphinoalcohols,[5] phosphinocarboxylates[6] and phosphine ethers.[3,7]

There have been relatively few reports, however, on studies of these phosphorus/oxygen systems with the early transition metals. Phosphorus/oxygen ligand complexes with iron-(II), -(III),[8] chromium,[3,9] molybdenum,[3,9,10] tungsten[3,9a–c,10e] and manganese[9,10e] have been reported, but are relatively few, and many of these reports show that no oxygen chelation to the metal has occurred. To our knowledge, there is only one example of a Group 4 metal complex with chelating oxygen/phosphorus ligands.[11] There is also a report of complexes of a phosphine phenol with Ti and Zr^{IV},[12] but only co-ordination through the oxygen was observed.

We are interested in applications of complexes with ether phosphines in the catalysis of reactions with alkenes. Complexes with electropositive metals have been shown to exhibit catalytic behaviour in a variety of reactions,[13,14] and recent reports have shown some titanium,[15] zirconium,[16] molybdenum[17,18] and tungsten[17,18] complexes to act as catalysts in Diels–Alder reactions. Additionally, ether phosphine complexes have been reported to show catalytic behaviour in a number of systems.[3] We have recently reported the preparation of the potentially terdentate ligand benzylbis(2-ethoxyethyl)phosphine (L) and its complexes of the nickel triad,[19] and also its reactivity with the cobalt-group metals.[20] Here we describe the preparation and characterisation of complexes with some early transition metals, and reactions of selected complexes with cyclohexene.

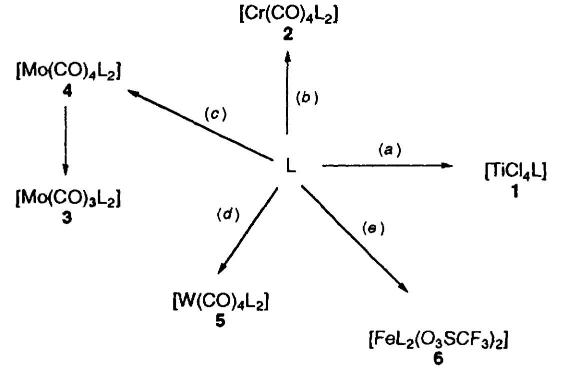

Scheme 1 L = $Ph_2CH_2P(CH_2CH_2OEt)_2$. (*a*) $TiCl_4$, light petroleum; (*b*) either (*i*) [$Cr(MeCN)_3(CO)_3$]–CH_2Cl_2 or (*ii*) [$Cr(MeCN)_2(CO)_4$]–CH_2Cl_2; (*c*) [$Mo(CO)_3(C_6H_3Me_3$-2,4,6)]–CH_2Cl_2; (*d*) [$W(CO)_3$-($C_6H_3Me_3$-2,4,6)]–C_6H_5Me, 100 °C; (*e*) $FeCl_2 \cdot 4H_2O$–AgO_3SCF_3–CH_2Cl_2

Results and Discussion

The NMR spectroscopic data for the new compounds discussed are collected in Table 1.

Titanium complexes

Addition of phosphine L to a solution of $TiCl_4$ in light petroleum (b.p. 40–60 °C) affords an air-sensitive red precipitate of [$TiCl_4L$] **1** (Scheme 1). Microanalysis indicates the proposed formulation, and ^{31}P-{^1H} NMR spectroscopy shows a sharp singlet at δ 26.2. A small quantity of impurity can sometimes be observed at *ca.* δ 10, which can be eliminated by recrystallisation. The ^1H NMR spectrum can be assigned on the basis of chemical shifts and signal intensities; two multiplets are seen at δ 1.9 and 2.3 which are attributed to PCH_2CH_2 protons of the non-chelating and chelating arms respectively. The resonances of the OCH_2CH_2 and OCH_2CH_3 protons of the chelating and non-chelating ether arms are coincident and

Table 1 NMR Spectroscopic data (δ, J/Hz)[a]

Complex	^{31}P-{^{1}H}	^{1}H	^{13}C-{^{1}H}
1	26.2 (s)	1.4 (t, $^3J_{HH}$ = 7, CH$_3$), 1.9 (m, PCH_2CH$_2$, non-chelate), 2.3 (m, PCH_2CH$_2$, chelate), 3.8 (d, J = 8, PhCH_2P), 4.1 (q, $^3J_{HH}$ = 7, OCH_2CH$_3$), 4.2 (m, OCH_2CH$_2$), 7.4 (m, aryl)	14.2 (s, CH$_3$), 24.7 (s, PCH$_2$CH$_2$, non-chelate), 25.5 (s, PCH$_2$CH$_2$, chelate), 33.6 (d, br, J = 12, PhCH$_2$P), 68.7 (s, OCH$_2$CH$_3$), 71.4 (s, OCH$_2$CH$_2$), 127.1, 128.6, 129.7, 129.9 (s, aryl)
2	41.8 (s)	1.2 (t, $^3J_{HH}$ = 7, CH$_3$), 2.0, 2.2 (m, br, PCH_2CH$_2$), 3.4 (d, separation of peaks = 5 Hz, PhCH_2P), 3.5 (q, $^3J_{HH}$ = 7, OCH_2CH$_3$), 3.7–3.8 (m, br, OCH_2-CH$_2$), 7.2–7.3 (m, aryl)	15.1 (s, CH$_3$), 30.1 (m, br, PCH$_2$CH$_2$), 39.4 (d, separation of peaks = 7 Hz, PhCH$_2$P), 66.1 (s, OCH$_2$CH$_3$), 66.2 (s, br, OCH$_2$CH$_2$), 126.3, 128.3, 130.1 (s, aryl), 223.1 ('t', CO)
3[b]	13.1 (s, br, $\nu_{\frac{1}{2}}$ = 102 Hz)	1.3 (m, br, CH$_3$), 1.8–2.4 (m, br, PCH_2CH$_2$, PhCH_2P), 3.4–4.2 (m, br, OCH_2CH$_2$), OCH_2CH$_2$), 7.1–7.5 (m, aryl)	15.4 (s, CH$_3$), 29.1 (d, br, $^2J_{PH}$ = 16.5, PCH_2CH$_2$), 38.2 (s, br, PhCH_2), 68.8 (s, br, OCH$_2$), 126.0–136.4 (m, aryl), 224 (m, br, CO)
5[b]	−5.9 ($^1J_{WP}$ = 136.7)	1.2 (t, $^3J_{HH}$ = 7, CH$_3$), 2.0–2.2 (m, PCH_2CH$_2$), 3.5 (m, PhCH_2P, OCH_2CH$_3$), 3.75 (m, br, OCH_2CH$_2$), 7.2–7.3 (m, aryl)	14.3 (s, br, CH$_3$), 30.6 (t, br, PCH$_2$CH$_2$), 40.8 (m, br, PhCH_2P), 65.5 (s, br, OCH$_2$CH$_3$), 66.7 (s, br, OCH_2CH$_2$), 126–135 (m, aryl), 203.8 (m, br, CO)
6[c]	11.3 (s, br, $\nu_{\frac{1}{2}}$ = 43 Hz)	*d*	14.3 (s, br, CH$_3$), 39.7 (s, br, PCH$_2$), 63.3, 66.3 (m, br, OCH$_2$), 119–129 (br, aryl), 150.5 (s, br, CF$_3$SO$_3$)

[a] In CDCl$_3$ unless otherwise stated. All at room temperature. Variable-temperature studies are detailed in the text and figures. [b] In C$_6$D$_6$. [c] ^{19}F: δ 1.75 (s, br, $\nu_{\frac{1}{2}}$ = 644 Hz, CF$_3$SO$_3$). [d] Broad.

Table 2 Selected bond lengths (Å) and angles (°) for [TiCl$_4$L] **1**

Ti–O(2)	2.189(3)	Ti–P	2.587(2)
Ti–Cl(1)	2.280(2)	Ti–Cl(3)	2.219(2)
Ti–Cl(2)	2.291(2)	Ti–Cl(4)	2.300(2)
O(2)–Ti–Cl(3)	167.03(8)	O(2)–Ti–Cl(1)	88.97(9)
Cl(3)–Ti–Cl(1)	103.98(7)	O(2)–Ti–Cl(2)	84.75(8)
Cl(3)–Ti–Cl(2)	94.44(6)	Cl(1)–Ti–Cl(2)	96.27(6)
O(2)–Ti–Cl(4)	84.57(8)	Cl(3)–Ti–Cl(4)	93.54(6)
Cl(1)–Ti–Cl(4)	94.36(6)	Cl(2)–Ti–Cl(4)	164.77(5)
O(2)–Ti–P	76.37(9)	Cl(3)–Ti–P	90.69(7)
Cl(1)–Ti–P	165.31(5)	Cl(2)–Ti–P	81.62(6)
Cl(4)–Ti–P	85.33(6)		

Table 3 Atomic coordinates (× 10^4) for complex **1**

Atom	x	y	z
Ti	4185(1)	2072(1)	1309(1)
Cl(1)	2465(1)	3847(2)	1172(1)
Cl(2)	3460(1)	564(1)	1996(1)
Cl(3)	5493(1)	3799(1)	1767(1)
Cl(4)	5057(1)	2825(1)	556(1)
P	5786(1)	−546(1)	1341(1)
O(1)	8068(2)	441(4)	2099(1)
O(2)	3248(2)	−64(4)	865(1)
C(1)	9985(4)	1999(7)	2188(2)
C(2)	8728(4)	1774(6)	2399(2)
C(3)	6939(4)	−116(6)	2318(2)
C(4)	6284(4)	−1464(5)	1958(1)
C(5)	7179(3)	−306(6)	967(2)
C(6)	7885(3)	−2032(6)	878(2)
C(7)	8772(4)	−2663(6)	1233(2)
C(8)	9426(4)	−4231(7)	1151(2)
C(9)	9196(4)	−5199(7)	706(2)
C(10)	8332(4)	−4604(7)	353(2)
C(11)	7661(4)	−3018(6)	436(2)
C(12)	4850(4)	−2317(5)	1034(2)
C(13)	3989(4)	−1455(5)	633(2)
C(14)	1959(3)	−648(6)	942(2)
C(15)	1179(4)	−452(7)	457(2)

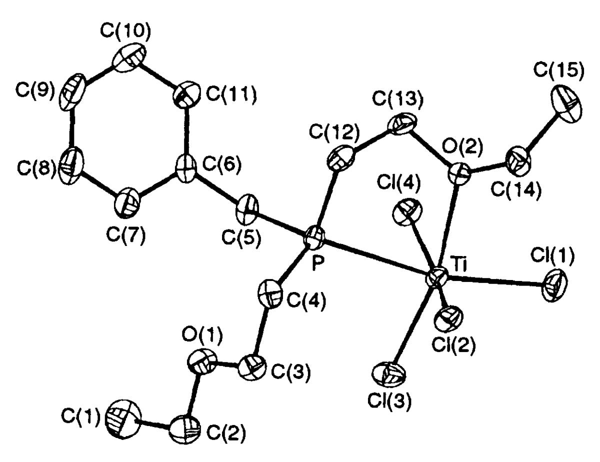

Fig. 1 Solid-state structure of [TiCl$_4$L] **1**

occur at δ 4.2 and 4.1 respectively. The ^{13}C-{^{1}H} NMR spectrum can also be assigned by chemical shifts and signal intensities, but it does not distinguish between chelating and non-chelating ether functions. The ^{31}P-{^{1}H} NMR spectra are invariant with temperature (−60 to +60 °C) indicating that **1** is non-fluxional in solution. Variable-temperature ^{1}H NMR spectra show no apparent change except for a slight broadening at lower temperatures (< −40 °C) which may be caused by a loss of resolution.

Mass spectrometry shows a small peak for $M^+ + 1$ (m/z 459), and extensive fragmentation is observed; the base peak is at m/z 77 (Ph) and 93 (PhCH$_2$ + 1) for the electron impact (EI) and chemical ionisation (CI) spectra respectively. Solid-state IR spectroscopy (Nujol mull) shows a relatively broad peak at 1101 cm^{-1} [ν_{asym}(C$_2$O)] which sharpens and shifts to higher frequencies (1107 cm^{-1}) on exposure to air. Peaks caused by the uptake of water are also observed 3500 (br) and 1600 cm^{-1}. This implies that the two peaks expected for ν_{asym}(C$_2$O) for the two ether arms (chelating and non-chelating) are hidden by the broadness of this peak. As complex **1** decomposes in air one of the peaks disappears (chelating ether) to leave one sharper peak at higher frequencies which is assigned to non-chelating ether functions. This is confirmed by the solution IR (CCl$_4$) spectrum where two peaks are observed (1108 and 1078 cm^{-1}); the peak at lower frequency is assigned to the chelating ether function, as has previously been observed for similar complexes.[3,20,21] Complex **1** is stable when stored under nitrogen as a solid or in solution, but is hygroscopic in air, decomposing to a colourless oil within 1 h.

The single-crystal structure for complex **1** has been determined (Fig. 1). Selected bond lengths and angles are in Table 2 and atomic coordinates are in Table 3. It confirms the stoichiometry indicated by NMR, IR and microanalysis data, where the titanium centre has a distorted-octahedral geometry, with an P,O-chelating ligand. Bond lengths are within expected values,[22] and the phosphorus has a higher *trans* influence than oxygen, since the bond *trans* to phosphorus [Ti–Cl(1) 2.280(2) Å] is longer, and therefore weaker, than that *trans* to oxygen [Ti–Cl(3) 2.219(2) Å]. The chelate bite angle shows a little strain, where the O(2)–Ti–P bond angle [76.37(9)°] is slightly lower than expected values.[23]

Complex **1** is the first titanium ether phosphine complex to be isolated and structurally characterised. Only one other structural characterisation of a titanium complex with a chelating oxygen/phosphorus ligand has been reported, a titanium(III) phosphino alkoxide ($^-OCBu^t{}_2CH_2PMe_2$).[11]

It should be noted that the same product is obtained when 2 mol equivalents of L are added, indicating that **1** is preferentially formed over the bis(phosphine) adduct. It may also be prepared using [$TiCl_4(thf)_2$] (thf = tetrahydrofuran) as starting material, but this results in larger quantities of the impurity (δ_P 10), and lower yields of **1**.

Complex **1** does not react with cyclohexene, and variable-temperature $^{31}P-\{^1H\}$ NMR spectroscopy on an *in situ* reaction confirms no alkene co-ordination to the metal. Also, **1** does not react with $NaBPh_4$, but addition of $AgBF_4$ or AgO_3SCF_3 to solutions of **1** results in the formation of pale yellow air-sensitive oils. Crystallisation of these oils was not possible, but spectroscopy and conductivity measurements indicate the composition of these oils may be [$TiCl_3L$]BF_4* and [$TiCl_3L$][O_3SCF_3]† respectively. Solution conductivity measurements (in nitromethane) indicate that the oils are both salts. The former appears to be a 1 : 1 electrolyte (Λ = 97.7 Ω^{-1} cm^2 mol^{-1}), whilst the latter is a partial conductor (Λ = 46.5 Ω^{-1} cm^2 mol^{-1}), possibly due to an interaction between the two ions as a close ion pair. Infrared spectroscopy is inconclusive, although data for the triflate salt indicate that both co-ordinating and non-co-ordinating triflate is present in solution, which is consistent with conductivity measurements.

The $^{31}P-\{^1H\}$ NMR spectra for these complexes exhibit a sharp singlet for both [$TiCl_3L$][BF_4] (δ 10.3) and [$TiCl_3L$][O_3SCF_3] (δ 11.1). The ^1H and $^{13}C-\{^1H\}$ spectra can be assigned on the basis of chemical shifts and signal intensities, but cannot distinguish the co-ordinating mode of the L ligand. The ^{19}F spectra may also be assigned according to chemical shift, with both species showing a singlet at room temperature (the triflate exhibits a broad singlet with $\nu_{\frac{1}{2}}$ = 195 Hz). The $^{31}P-\{^1H\}$, ^1H and ^{19}F NMR spectra are temperature invariant, though the ^{19}F spectrum for the triflate complex appears to broaden slightly at low temperatures. Although there is evidence for triflate co-ordination from IR spectroscopic data, a fluxional process or ligand lability cannot be readily distinguished using variable-temperature NMR spectroscopy.

Chromium complexes

Addition of a standard solution of phosphine L to [$Cr(MeCN)_3(CO)_3$] enables the isolation of [$Cr(CO)_4L_2$] **2** in poor yield (27%). The stoichiometry is inferred from microanalysis and mass spectrometry, where a small peak due to the molecular ion is observed (*m/z* 700.0). Fragmentation to give CrL_2 (*m/z* 588) and CrL (320.5) occurs together with other peaks due to ligand fragments; the base peak is at *m/z* 91 (CH_2Ph). The $^{31}P-\{^1H\}$ NMR spectrum shows a sharp singlet at δ 41.8. The ^1H spectrum can be assigned on the basis of chemical shifts and signal intensities, as can the $^{13}C-\{^1H\}$ spectrum where a weak apparent triplet is observed at δ 223 (CO). The IR spectrum data (solid state) shows an absorption at 1092 cm^{-1} assigned to $\nu_{asym}(C_2O)$, and two peaks in the carbonyl region (1878 and 1856 cm^{-1}). This is in agreement with data for other complexes of the type [$Cr(CO)_4(PR_3)_2$] for which the two peaks at higher frequency (*ca.* 2000 cm^{-1}) are often very weak and may not be observed.[24] Solution IR spectroscopy is relatively uninformative where both of these absorptions are large and broad. The $^{31}P-\{^1H\}$ NMR spectra are invariant in the range +30 to −80 °C. Similarly, ^1H NMR spectra show little difference except for a broadening below −20 °C. Complex **2** is air-stable in the solid or solution states, indicating that no ether co-ordination occurs. The complex probably has *cis* (monodentate) phosphines.

In order to confirm the composition of complex **2**, the reaction of the bis(acetonitrile) complex [$Cr(MeCN)_2(CO)_4$] with L was examined. The addition of 1 or 2 mole equivalents of L to this complex affords **2**, and in the latter case in good yield (84%). This is consistent with the proposed structure of **2**, where preparation from [$Cr(MeCN)_3(CO)_3$] requires a proportionation of starting material, giving a maximum possible yield of 75%. This reaction is surprising, showing that the chromium will go to extraordinary lengths to avoid chelation through the oxygen; similar reactions have previously been observed for complexes of this type.[9c] Reaction of [$Cr(MeCN)_3(CO)_3$] with an excess of L, both with and without heating, affords **2** plus free phosphine, indicating that it is not possible to form the tris(phosphine) complex [$Cr(CO)_3L_3$], possibly due to the steric bulk of L.

Thermal or UV-activated carbonyl elimination from complex **2**, in order to encourage chelation, was attempted, but no reaction was observed. The reaction of **2** with trimethylamine *N*-oxide in dichloromethane was also attempted, but no discrete and readily identifiable product could be isolated.

Molybdenum complexes

The reaction of [$Mo(CO)_3(C_6H_3Me_3$-2,4,6)] with 2 mol of L resulted in the isolation of the complex [$Mo(CO)_3L_2$] **3**. This stoichiometry is indicated by microanalysis, and $^{31}P-\{^1H\}$ NMR spectroscopy shows a broad singlet at δ 13.1 ($\nu_{\frac{1}{2}}$ = 102 Hz). The ^1H NMR spectrum is relatively broad and uninformative, as is the $^{13}C-\{^1H\}$ spectrum, where a weak and broad resonance assigned to CO is observed at δ 224 which does not sharpen at low temperature (−40 °C). The IR spectrum shows the presence of L with a broad absorption at 1103 cm^{-1} [$\nu_{asym}(C_2O)$], and three carbonyl peaks at 1912, 1827 and 1778 cm^{-1}, indicating three different CO groups. The CO peak at 1778 cm^{-1} indicates a co-ordinating ether, since it is shifted to considerably lower frequencies from normal values.[9c] This may be expected since the ether would have no capacity for π-back bonding, so the relative back-bonding ability of this CO group *trans* to ether is comparatively greater than those *trans* to phosphine (which can undergo back bonding with the metal).

Variable-temperature $^{31}P-\{^1H\}$ NMR spectra of complex **3** have been measured ($C_6D_5CD_3$, −80 to +80 °C). At low temperatures **3** exhibits two sharp singlets (δ 26.7 and 10.2) indicating two different phosphorus environments. As the

---

* IR: ν_{max}/cm^{-1} (Nujol) 1100 [br, $\nu_{asym}(C_2O)$], 1022, 1259 [$\nu(BF_4)$], 400 [ν(Ti–Cl)]; $\nu(CCl_4)$ 1106, 1075 [$\nu_{asym}(C_2O)$], 1032, 1261 [$\nu(BF_4)$]; $\delta_P(CDCl_3)$ 10.3 (s); $\delta_H(CDCl_3)$ 1.2 (t, $^3J_{HH}$ = 6 Hz, CH_3), 2.7 (m, br, PCH_2CH_2), 3.5 (d, br, separation of lines = 4 Hz, $PhCH_2P$), 3.8 (t, br, OCH_2CH_2, OCH_2CH_3) and 7.3–7.4 (m, br, aryl); δ_C 14.75 (s, CH_3), 18.0 (s, PCH_2CH_2), 20.2 (s, $PhCH_2P$), 63.4, 63.6 (s, OCH_2CH_3), 66.6 (s, OCH_2CH_2) and 128–130 (m, aryl); δ_F −149.1 (s); *m/z* (EI) 508 (M^+, < 1%), 91 (CH_2Ph, 100), 122 (PCH_2Ph, 50), 150 ($PhCH_2PCH_2CH_2$, 15), 196 (L − CH_2CH_2OEt, 10), 268.5 (L, 5), plus other ligand fragments.

† IR: ν_{max}/cm^{-1} (Nujol) 1096 [br, $\nu_{asym}(C_2O)$], 1300 (br), 1261 [$\nu_{asym}(CF_3)$], 1234, 1215 [br, $\nu_{sym}(CF_3)$], 1029 [$\nu_{asym}(SO_3)$], 638 [ν(CS)], 419 [ν(Ti–Cl)]; (CCl_4) 1106, 1075 [$\nu_{asym}(C_2O)$], 1354, 1335, 1261 [$\nu_{asym}(CF_3)$], 1237, 1226, 1204 [$\nu_{sym}(CF_3)$], 1166 [$\nu_{sym}(SO_3)$], 1029 [$\nu_{asym}(SO_3)$], 638 [ν(CS)]; $\delta_P(CDCl_3)$ 11.1 (s); $\delta_H(CDCl_3)$ 1.2 (t, $^3J_{HH}$ = 7 Hz, CH_3), 2.6 (q, separation of peaks = 6 Hz, PCH_2CH_2), 3.5 (dq, separation of peaks = 4, 1.5 Hz, OCH_2CH_3), 3.75 (d, separation of peaks = 4 Hz, $PhCH_2P$), 3.8 (m, OCH_2CH_2) and 7.3–7.4 (m, aryl); $\delta_C(CDCl_3)$ 14.75 (s, CH_3), 17.9 (s, PCH_2CH_2), 20.05 (s, br, $PhCH_2P$), 63.25, 62.5 (br, OCH_2CH_3), 66.85 (s, OCH_2CH_2) and 128–130 (m, aryl, CF_3SO_3); $\delta_F(CDCl_3)$ −75.5 (s, br, $\nu_{\frac{1}{2}}$ = 195 Hz); *m/z* (EI) 571.3 (M^+, < 1%), 65 (45), 91 (CH_2Ph, 100), 121 (PCH_2Ph, 5), plus other ligand fragments.

solution is warmed (−40 °C), the resolution improves and P–P coupling is observed ($^2J_{PP}$ = 25.7 Hz) which is consistent with *cis* phosphines.[25] As the solution is warmed further the signal broadens to a broad singlet; coalescence is observed at *ca.* 4 °C. At higher temperatures (> 60 °C) it appears as a sharp singlet at δ 18.3, indicating a fluxional process involving free exchange between the two phosphorus atoms (Scheme 2); $\Delta G^{\ddagger}$ for this process is estimated at 53 ± 2 KJ mol^{-1}. Variable-temperature ^{1}H NMR spectra are broad and uninformative.

The single-crystal structure of complex **3** has been determined (Fig. 2), and confirms the stoichiometry indicated by ^{31}P-{^{1}H} NMR and Fourier-transform spectroscopy. Selected bond angles and lengths are in Table 4 and atomic co-ordinates in Table 5. The molybdenum centre has a *fac* arrangement of ligands and a distorted-octahedral geometry [C(33)–Mo–O(3) 96.06(12)°], with *cis* phosphorus atoms. One ligand is shown to bond only through the phosphorus atom, whilst the other ligand is P,O bonding. As expected, the metal–carbonyl bond *trans* to oxygen [Mo–C(31) 1.914(4) Å] is considerably shorter than those *trans* to phosphorus [Mo–C(32) 1.968(4), Mo–C(33) 1.964(4) Å], which reflects the inability of the oxygen to act as a π acceptor. There is negligible difference between the two metal–phosphorus bond lengths. Bond lengths and angles are within expected values,[9c,10b] however the chelate bite angle [P(2)–Mo–O(3) 74.79(7)°] shows a little strain compared with those of similar complexes.[23]

Crystallographically determined molybdenum ether phosphine complexes with chelating P,O groups are rare; there is only one other, *i.e.* [Mo(CO)$_3${P[C$_6$H$_2$(OMe)$_3$-2,4,6]$_3$}].[10b]

It is interesting that ^{31}P-{^{1}H} NMR spectroscopy on the oleaginous residue initially prepared, prior to work-up, shows a sharp singlet at δ 2. The IR spectrum of this oil shows only two peaks in the CO region (1931 and 1831 cm^{-1}), indicating that no ether co-ordination has occurred.[9c] These data lead to the tentative formulation of this oil as [Mo(CO)$_4$L$_2$] **4**. On work-up a carbonyl group is dissociated, allowing ether co-ordination to the metal and affording **3** in relatively poor yield (36%).

Tungsten complexes

Reaction of [W(CO)$_3$(C$_6$H$_3$Me$_3$-2,4,6)] with L (100 °C, 7 d) affords yellow crystals of [W(CO)$_4$L$_2$] **5** in poor yield. Microanalysis indicates the proposed formulation, and ^{31}P-{^{1}H} NMR spectroscopy shows a singlet at δ −5.9, with attendant ^{31}P–^{183}W coupling (^{183}W, 14.3% abundance; $^1J_{WP}$ = 136.7 Hz). This is very low in comparison with other tungsten ether phosphine complexes,[9c,10e] and indicates a weak interaction between the metal and phosphine. The chemical shift at relatively high field (δ −5.9) indicates no chelation, since chelation tends to cause a significant downfield chemical shift.[10b,26] The proton and ^{13}C-{^{1}H} NMR spectra can be assigned on the basis of chemical shifts and signal intensities, where, in the latter, a weak and broad multiplet due to CO may be seen (δ 203.8). Infrared spectroscopy confirms the proposed formulation; only two peaks may be assigned to CO (1881 and 1856 cm^{-1}). This is very similar to the chromium (**2**) and molybdenum (**4**) analogues. For the molybdenum complex with chelating ether a stretch at lower frequency (1778 cm^{-1}) is observed; this peak is absent for **5**, indicating no ether co-ordination. Only one peak assigned to ν_{asym}(C$_2$O) in L is observed (1103 cm^{-1}), again indicating no ether co-ordination.

Scheme 2

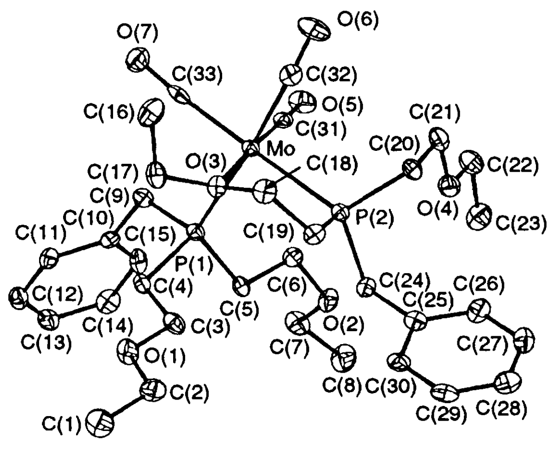

Fig. 2 Solid-state structure of [Mo(CO)$_3$L$_2$] **3**

Mass spectrometry also supports the proposed formulation, there being a small peak assigned to M^+ (*m*/*z* 832). A small peak due to dissociation of one CO group [W(CO)$_3$L$_2$, *m*/*z* 804] may also be seen, and extensive fragmentation of the ligand occurs; the base peak is at *m*/*z* 91 (CH$_2$Ph). Complex **5** is non-fluxional in solution (^{31}P-{^{1}H} NMR spectroscopy, −90 to +60 °C). Variable-temperature ^{1}H NMR spectra are broad and uninformative.

Thermal or UV-activated carbonyl abstraction from complex **5**, in order to encourage chelation, resulted in no reaction. If the reaction between L and [W(CO)$_3$(C$_6$H$_3$Me$_3$-2,4,6)] is undertaken under less vigorous conditions (*e.g.* lower temperatures, photolysis) then it is either very slow or does not occur. The isolation of **5** again indicates the unusually high reluctance of L to chelate through the ether function. The reactions of all the Group 6 metals show that the formation of chelates is not preferred, and all tricarbonyl precursors readily proportionate to yield complexes of the type [M(CO)$_4$L$_2$].

Iron complexes

Addition of phosphine L to either FeCl$_2$·4H$_2$O or FeCl$_2$ affords a brown oil from which no discrete and readily identifiable products could be isolated. Addition of silver triflate to a solution of this oil again does not enable isolation of a discrete complex although a reaction may be seen to occur. If, however, chloride is abstracted prior to the addition of L, by the reaction of silver triflate with FeCl$_2$·4H$_2$O (in ethanol), followed by addition of L to the filtered solution, pale green prisms of [FeL$_2$(O$_3$SCF$_3$)$_2$] **6** are isolated in good yield. Microanalysis indicates the proposed stoichiometry, and the ^{31}P-{^{1}H} NMR spectrum exhibits a singlet at δ 11.3 ($\nu_{\frac{1}{2}}$ = 43 Hz). The ^{1}H NMR spectrum is broad and uninformative, as is the ^{13}C-{^{1}H} spectrum, where a broad resonance at δ 150.5 assigned to triflate is observed. A broad singlet is observed in the ^{19}F NMR spectrum at δ 1.75 ($\nu_{\frac{1}{2}}$ = *ca.* 640 Hz), again assigned to triflate.

Table 4 Selected bond lengths (Å) and angles (°) for *fac*-[Mo(CO)$_3$-L$_2$] **3**

Mo–P(1)	2.534(1)	Mo–P(2)	2.538(1)
Mo–O(3)	2.331(2)	Mo–C(31)	1.914(4)
Mo–C(32)	1.968(4)	Mo–C(33)	1.964(4)
C(31)–Mo–C(33)	87.8(2)	C(31)–Mo–C(32)	86.62(14)
C(33)–Mo–C(32)	86.1(2)	C(31)–Mo–O(3)	176.2(1)
C(33)–Mo–O(3)	96.06(12)	C(32)–Mo–O(3)	93.76(12)
C(31)–Mo–P(1)	87.53(11)	C(33)–Mo–P(1)	88.83(11)
C(32)–Mo–P(1)	172.4(1)	O(3)–Mo–P(1)	92.40(6)
C(31)–Mo–P(2)	101.4(1)	C(33)–Mo–P(2)	169.0(1)
C(32)–Mo–P(2)	88.32(11)	O(3)–Mo–P(2)	74.79(7)
P(1)–Mo–P(2)	97.59(3)		

Table 5 Atomic coordinates (× 10^4) for complex **3**

Atom	*x*	*y*	*z*	Atom	*x*	*y*	*z*
Mo	1503(1)	1813(1)	2660(1)	C(13)	3526(4)	−1305(2)	4438(2)
P(1)	1939(1)	722(1)	2709(1)	C(14)	2419(4)	−1070(2)	4591(2)
P(2)	−272(1)	1800(1)	1310(1)	C(15)	2197(4)	−477(2)	4429(2)
O(1)	3282(2)	312(1)	278(2)	C(16)	4200(4)	2592(2)	1527(3)
O(2)	−1379(2)	−36(1)	3050(2)	C(17)	3710(4)	1984(2)	1277(3)
O(3)	2403(2)	1936(1)	1272(2)	C(18)	1693(3)	2283(2)	537(2)
O(4)	−2603(2)	1837(1)	2265(2)	C(19)	489(3)	1979(2)	254(2)
O(5)	153(3)	1631(1)	4429(2)	C(20)	−1382(3)	2393(2)	1339(2)
O(6)	1038(3)	3151(1)	2975(2)	C(21)	−2013(4)	2389(2)	2226(3)
O(7)	3890(3)	2033(1)	4085(2)	C(22)	−3174(4)	1766(2)	3109(3)
C(1)	3868(4)	103(2)	−1235(3)	C(23)	−3737(4)	1158(2)	3062(3)
C(2)	2865(4)	341(2)	−711(2)	C(24)	−1197(3)	1156(2)	852(2)
C(3)	2364(3)	463(2)	844(2)	C(25)	−2104(4)	1238(2)	−36(2)
C(4)	2918(3)	408(2)	1888(2)	C(26)	−3290(4)	1428(2)	10(3)
C(5)	646(3)	207(2)	2586(2)	C(27)	−4107(4)	1513(2)	−808(3)
C(6)	−381(3)	363(2)	3167(2)	C(28)	−3770(4)	1395(2)	−1688(3)
C(7)	−1140(4)	−576(2)	3548(3)	C(29)	−2584(4)	1206(2)	−1755(3)
C(8)	−2318(4)	−902(2)	3510(3)	C(30)	−1752(4)	1131(2)	−931(3)
C(9)	2801(3)	521(2)	3884(2)	C(31)	662(4)	1701(2)	3747(3)
C(10)	3066(3)	−114(2)	4090(2)	C(32)	1208(3)	2656(2)	2808(2)
C(11)	4184(3)	−368(2)	3949(2)	C(33)	3015(4)	1933(2)	3551(3)
C(12)	4414(4)	−951(2)	4128(2)				

Variable-temperature $^{31}P-\{^1H\}$ and ^{19}F NMR spectra show no change with temperature (−60 to +60 °C). Variable-temperature ^1H NMR spectra are broad and uninformative at all temperatures, and are temperature invariant. Complex **6** is diamagnetic, indicating an octahedral rather than a tetrahedral geometry (Fe^{II}, d^6) and presumably chelating (O,P) L ligands. The ESR spectra of frozen (100 K) solutions of **6** are silent indicating the absence of paramagnetic species, and therefore the broadness in the NMR spectra appears not to be caused by traces of an iron(III) impurity. It follows that it must be caused by a fluxional process that cannot be identified by variable-temperature NMR spectroscopy.

Solid-state IR spectroscopy (Nujol mull) shows the presence of L [$\nu_{asym}(C_2O)$ 1103 cm^{-1}] and triflate. The triflate bands are not split; any fine structure may be obscured by the broadness of the peaks. The peak attributed to $\nu_{asym}(CF_3)$ (1260 cm^{-1}) is broad. In solution (CCl_4) the spectrum is better resolved, and the peak assigned to $\nu_{asym}(C_2O)$ in L is split into two (1122 and 1108 cm^{-1}), indicating the presence of both co-ordinated and non-co-ordinated ether functions. The absorption assigned to $\nu_{asym}(CF_3)$ is also split, and bands are observed at 1212, 1238 and 1322 cm^{-1}. A recent report[27] states that triflate peaks split on co-ordination to the metal, and this has previously been observed for the cobalt(II) analogue of **6**.[20] In this complex it is unclear whether ether co-ordination occurs since any fine structure may be obscured by the broadness of the peaks. It has also been reported that the peak attributed to $\nu_{asym}(CF_3)$ shifts to higher frequencies (> 1300 cm^{-1}) on co-ordination to the metal,[28] and since bands are observed both above and below 1300 cm^{-1} co-ordinating and non-co-ordinating triflate may be present in solution.

Solution conductivity measurements in both dichloromethane and ethanol indicate partial dissociation of triflate. In nitromethane, however, full dissociation of triflate occurs to give a three-ion species ($\Lambda = 207.6\ \Omega^{-1}\ cm^2\ mol^{-1}$), corresponding to $[FeL_2]^{2+}2CF_3SO_3^-$. The $^{31}P-\{^1H\}$ NMR spectrum for **6** in nitromethane exhibits a singlet at δ 11.3 as before; **6** is diamagnetic in nitromethane, indicating that it has an octahedral geometry with terdentate chelating L ligands (Scheme 3). This is the first example where these L ligands bind in such a manner.

The single-crystal structure of complex **6** has been determined and is shown in Fig. 3; selected bond angles and lengths are in Table 6 and atomic co-ordinates in Table 7. The iron(II) centre has a distorted-octahedral geometry, with *trans*-chelating ligands (P,O) and *trans*-co-ordinating triflates. The Fe–O bond lengths are within expected values.[8c,29] However, the Fe–P bond length is considerably longer than expected for a low-spin octahedral iron(II) complex,[8c,30] indicating a relative weakening of this bond. Compression of the O(2)–Fe–P(1) bond angle [78.94(9)°] shows chelate ring strain within the molecule, and is close to expected values.[23]

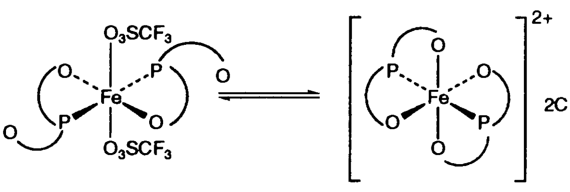

Scheme 3

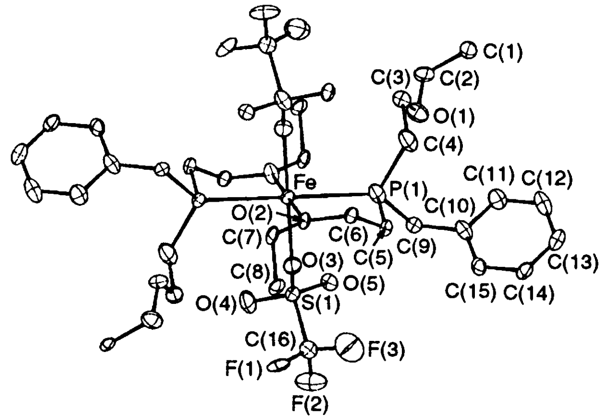

Fig. 3 Solid-state structure of $[FeL_2(O_3SCF_3)_2]$ **6**

There are significant differences between the angles around the co-ordinated donors with a significant compression of the Fe–P(1)–C(12) angle [95.0(2)°] compared with other unrestricted tertiary phosphine phosphorus centres and with the less-restricted non-chelating ether arms. This indicates a rotation about the Fe–P bond, so that maximum Fe–O bonding may occur at the expense of Fe–P bonding, as has been observed in the isostructural cobalt(II) analogue.[20] This strongly indicates that the distortion in the cobalt complex is caused by structural effects imposed by the chelating ligand

Table 6 Selected bond lengths (Å) and angles (°) for $[FeL_2(O_3SCF_3)_2]$ **6***

Fe–P(1)	2.583(2)	Fe–O(3)	2.060(3)
Fe–O(2)	2.190(3)		
O(3)–Fe–O(3^I)	180.0	O(2)–Fe–P(1^I)	101.1(1)
O(3^I)–Fe–O(2)	87.83(13)	P(1)–Fe–P(1^I)	180.0
O(3)–Fe–O(2)	92.17(13)	C(4)–P(1)–Fe	120.9(2)
O(3)–Fe–P(1)	92.05(11)	C(7)–O(2)–Fe	126.7(3)
O(2)–Fe–P(1)	78.94(9)	C(5)–P(1)–Fe	96.1(2)
O(3)–Fe–P(1^I)	87.95(11)	C(6)–O(2)–Fe	119.8(3)

* Symmetry transformation used to generate equivalent atoms I $-x, -y, -z$.

Table 7 Atomic coordinates (× 10⁴) for complex **6**

Atom	*x*	*y*	*z*
Fe	0	0	0
F(1)	2436(3)	−1208(3)	2725(2)
F(2)	2248(3)	177(3)	3646(2)
F(3)	853(3)	−884(3)	3065(3)
S(1)	1416(1)	730(1)	2008(1)
P(1)	1788(1)	47(1)	−673(1)
O(1)	3414(3)	−2166(3)	−58(2)
O(2)	270(3)	1951(3)	−86(2)
O(3)	892(3)	−77(3)	1280(2)
O(4)	2470(3)	1199(3)	1898(3)
O(5)	655(3)	1544(3)	2294(3)
C(1)	5165(5)	−3184(5)	425(4)
C(2)	3943(5)	−3242(4)	328(4)
C(3)	3443(5)	−1215(4)	554(4)
C(4)	3148(4)	−27(4)	37(3)
C(5)	1701(4)	1644(4)	−980(4)
C(6)	1330(4)	2405(4)	−268(4)
C(7)	−425(5)	2892(4)	151(4)
C(8)	−986(5)	3585(5)	−671(5)
C(9)	1945(4)	−702(4)	−1736(3)
C(10)	2903(5)	−278(4)	−2147(3)
C(11)	3905(5)	−862(5)	−2000(3)
C(12)	4783(5)	−468(5)	−2362(4)
C(13)	4680(5)	557(5)	−2889(4)
C(14)	3698(5)	1141(5)	−3048(4)
C(15)	2809(5)	728(5)	−2691(4)
C(16)	1754(6)	−358(5)	2896(4)

rather than a Jahn–Teller distortion, which is precluded for Fe^{II}. Complex **6** does not react with cyclohexene, and variable-temperature $^{31}P-\{^1H\}$ NMR spectroscopy (−60 to +60 °C) on an *in situ* reaction confirms no alkene co-ordination.

Experimental

All syntheses described were carried out under strictly anaerobic conditions using a Halco Engineering 140 FF glove-box, or using standard vacuum-line techniques. All solvents were refluxed under N_2 over sodium–benzophenone and were distilled immediately prior to use, except for ethanol and dichloromethane which were dried over CaH_2 and toluene which was dried over sodium. The metal chlorides and silver salts were used as received. Bis(2-ethoxyethyl)benzylphosphine was prepared as previously described,[19] as were the starting materials $[M(CO)_3(MeCN)_3]$ (M = Cr, Mo or W) and $[Cr(CO)_4(MeCN)_2]$[31] and $[Mo(CO)_3(C_6H_3Me_3\text{-}2,4,6)]$.[32]

Photolyses were performed with a Hanovia 50W medium-pressure mercury lamp in quartz glassware. The NMR spectra were recorded on a Bruker WM-360 or AMX-360 spectrometer operating at 360.13 (^1H) or 90.56 MHz (^{13}C), or on a JEOL FX-90Q operating at 89.55 (^1H), 36.23 (^{31}P), 84.25 (^{19}F) or 22.49 MHz (^{13}C). They were referenced externally to 85% H_3PO_4 (^{31}P), CF_3CO_2H [^{19}F, δ −76.9 relative to $CFCl_3$ (δ 0)] or $SiMe_4$ (^1H), or internally to solvent carbons (C_6D_6, δ 128.0; $CDCl_3$, δ 76.9) (^{13}C) or residual protic impurity ($C_6D_5CD_3$, δ 7.09; C_6D_6, δ 7.15; $CDCl_3$, δ 7.27) (^1H). The ESR measurements were made on a Varian E3 spectrometer. Infrared spectral data were obtained from a Nicolet 510 FT-IR spectrometer in conjunction with a 620 processor or a Perkin-Elmer 577 grating spectrophotometer; solid-state spectra were run in Nujol mulls, solution spectra in CCl_4. Elemental analyses were performed in this department on a Perkin-Elmer 240C elemental analyser. Conductivity data were obtained from a PTI-18 digital conductivity meter, and referenced against a standard solution of 1 mol dm^{-3} KCl. Melting points were measured in sealed capillaries and are uncorrected. Yields quoted are based on the metal complex or metal halide precursors.

Preparations

[Benzylbis(2-ethoxyethyl)phosphine]tetrachlorotitanium(IV) 1. To a solution of $TiCl_4$ (0.25 cm³, 1.1 mmol) in light petroleum (50 cm³) was added a standard solution of L in light petroleum (1.1 cm³, 1.1 mmol), and the colourless solution allowed to stir for 2 h, during which time it turned orange and a red precipitate was formed. The solution was filtered and the residue washed with light petroleum (2 × 10 cm³), yielding **1** as an air sensitive orange powder in excellent yield (0.49 g, 98%). The complex was recrystallised as red prisms from dichloromethane or dichloromethane–light petroleum (2:1) [Found (Calc.): C, 39.2 (39.3); H, 5.8 (5.5)%]. M.p. 147–150 °C. *m/z* (EI) 77 (Ph, 100), 91 (CH_2Ph, 75), 122 (PCH_2Ph, 60%), plus other ligand fragments; (CI) 459 (M^+ + 1, < 1), 93 (CH_2Ph, 100%), plus other ligand fragments. IR/cm^{-1}: (solid state), 1101 (br) [$\nu_{asym}(C_2O)$], 400 [ν(Ti–Cl)]; (solution), 1108, 1078 [$\nu_{asym}(C_2O)$].

Bis[benzylbis(2-ethoxyethyl)phosphine]tetracarbonylchromium(0) 2. *Method* (*a*). To a solution of $[Cr(CO)_3(MeCN)_3]$ (0.44 g, 1.70 mmol) in dichloromethane (40 cm³) was added a standard solution of L in light petroleum (3.4 cm³, 3.40 mmol) and the mixture allowed to stir (2 d) affording an orange solution. The solvents were removed *in vacuo* and the residue was extracted into hot light petroleum (100 cm³). After concentration of this solution to saturation complex **2** was isolated in poor yield as yellow needles (0.32 g, 27%).

Method (*b*). As method (*a*), but using $[Cr(CO)_4(MeCN)_2]$ (0.18 g, 0.73 mmol). Reaction time = 1 h; yield = 0.43 g (84%) [Found (Calc.): C, 57.8 (58.3); H, 7.3 (7.2)%]. M.p. 68–69 °C. *m/z* (EI) 700.0 (M^+, < 1), 588 (M^+ − 4CO, 2), 320.5 (CrL, 3), 91 (CH_2Ph, 100%) plus various ligand fragments. IR/cm^{-1}: (solid state), 1878, 1856 [ν(CO)], 1092 [$\nu_{asym}(C_2O)$]; (solution), 1877 (br) [ν(CO)], 1103 (br) [$\nu_{asym}(C_2O)$].

Bis[benzylbis(2-ethoxyethyl)phosphine]tricarbonylmolybdenum(0) 3. To a solution of $[Mo(CO)_3(C_6H_3Me_3\text{-}2,4,6)]$ (0.31 g, 1.04 mmol) in dichloromethane (50 cm³) was added a standard solution of L in light petroleum (1.95 cm³, 2.07 mmol) and the solution allowed to stir (12 h). The solvents were removed *in vacuo* and the residue (complex **4**) was extracted into light petroleum (80 cm³). After concentration of this solution to saturation, yellow air-sensitive crystals of **3** were isolated as needles in moderate yield (0.27 g, 36%) [Found (Calc.): C, 55.2 (55.3); H, 7.4 (7.0)%]. IR/cm^{-1}: (solid state), 1912, 1827, 1778 [ν(CO)], 1103 (br) [$\nu_{asym}(C_2O)$].

Bis[benzylbis(2-ethoxyethyl)phosphine]tetracarbonyltungsten(0) 5. To a solution of $[W(CO)_3(C_6H_3Me_3\text{-}2,4,6)]$ (0.29 g, 0.75 mmol) in toluene (50 cm³) was added a standard solution of L in light petroleum (1.50 cm³, 1.5 mmol) and the solution allowed to stir (7 d, 100 °C) yielding an orange solution. The solvents were removed *in vacuo*, and the residue was extracted into hot light petroleum (80 cm³). The solution

Table 8 Crystal data for compounds **1**, **3** and **6***

	1	**3**	**6**
Empirical formula	$C_{15}H_{25}Cl_4O_2PTi$	$C_{33}H_{50}MoO_7P_2$	$C_{32}H_{50}F_6FeO_{10}P_2S_2$
M_r	458.02	716.61	890.63
a/Å	10.707(7)	10.983(5)	12.250(9)
b/Å	7.409(6)	22.819(9)	11.056(6)
c/Å	26.401(9)	14.141(6)	15.267(8)
β/°	92.35(5)	97.72(2)	100.441(10)
U/Å^3	2093(2)	3512(3)	2033(2)
Z	4	4	2
D_c/g cm^{-3}	1.454	1.355	1.455
F(000)	944	1504	928
μ/mm^{-1}	1.001	0.508	0.630
Crystal size/mm	0.145 × 0.145 × 0.07	0.22 × 0.07 × 0.07	0.14 × 0.14 × 0.1
No. reflections collected	7833	13662	7867
θ Range/°	1.90–25.03	1.78–25.09	2.29–25.11
hkl Ranges	−11 to 9, −8 to 8, −29 to 31	−12 to 11, −25 to 24, −11 to 15	−13 to 13, −12 to 12, −18 to 17
No. unique data	3097	5292	3061
R_{int}	0.1353	0.0514	0.0796
wR_2 (all data)	0.0931	0.0842	0.1234
($F_o > 4\sigma F_o$)	0.0885 (2184 data)	0.0789 (3175 data)	0.0816 (1238 data)
R_1 (all data)	0.0717	0.0582	0.0964
($F_o > 4\sigma F_o$)	0.0420	0.0357	0.0404
No. parameters	210	392	243
ρ_{max}, ρ_{min}/e Å^{-3}	0.435, −0.541	0.665, −0.346	0.45, −0.24

* Details in common: monoclinic, space group $P2_1/c$; $wR_2 = \{\Sigma[w(F_o^2 - F_c^2)^2]/\Sigma w(F_o^2)^2\}^{\frac{1}{2}}$; $R_1 = \Sigma(F_o - F_c)/\Sigma(F_o)$.

was filtered and after concentration to saturation, yellow needles of complex **5** were isolated in poor yield (0.19 g, 30%) [Found (Calc.): C, 49.0 (49.1); H, 6.6 (6.1)%]. M.p. 71–73 °C. m/z (EI) 832 (M^+, < 1), 804 [$W(CO)_3L_2$, < 1], 91 (CH_2Ph, 100%) plus various ligand fragments. IR/cm^{-1}: (solid state), 1881, 1856 [ν(CO)], 1097 (br) [$\nu_{asym}(C_2O)$]; (solution), 1876 (br) [ν(CO)], 1103 [$\nu_{asym}(C_2O)$].

Bis[benzylbis(2-ethoxyethyl)phosphine]bis(trifluoromethanesulfonato)iron(II) 6. To a solution of $FeCl_2{\cdot}4H_2O$ (0.60 g, 3.0 mmol) in ethanol (50 cm^3) was added silver triflate (1.55 g, 6.0 mmol), generating a yellow solution with a white precipitate (AgCl). This solution was filtered, a standard solution of L in light petroleum (5.8 cm^3, 6.0 mmol) added, and the solution allowed to stir (12 h), affording a green solution. The solvents were removed *in vacuo* and the residue was triturated with light petroleum (50 cm^3) (1 h) and then extracted into dichloromethane (50 cm^3). After filtration and concentration of this solution to saturation, pale green air-sensitive crystals of complex **6** were isolated as prisms in moderate yield (1.76 g, 65%) [Found (Calc.): C, 43.1 (43.2); H, 5.8 (5.7)%]. M.p. 147–148 °C. IR/cm^{-1}: (solid state), 1260 (br) [$\nu_{asym}(CF_3)$], 1220 (br) [$\nu_{sym}(CF_3)$], 1103 (br) [$\nu_{asym}(C_2O)$], 1031 (br) [$\nu_{asym}(SO_3)$], 1161 (br) [$\nu_{sym}(SO_3)$], 638 [ν(CS)]; (solution), 1322, 1260 (br) [$\nu_{asym}(CF_3)$], 1238, 1212 [$\nu_{sym}(CF_3)$], 1122, 1108 [$\nu_{asym}(C_2O)$], 1032 (br) [$\nu_{asym}(SO_3)$], 1174 (br) [$\nu_{sym}(SO_3)$], 638 [ν(CS)].

Crystallography

Crystals of complexes **1** and **6** suitable for X-ray work were recrystallised from dichloromethane; **3** was recrystallised from diethyl ether.

Data collection and processing.[33] Data were collected on a Delft Instruments FAST TV area detector diffractometer, X-rays being produced by a rotating-anode generator using a molybdenum target [λ(Mo-Kα) = 0.710 69 Å], and being controlled by a Micro Vax 3200 computer driven by MADNES[34] software. All data sets were recorded at 120 K using an Oxford cryostream low-temperature cooling system. Data reduction was performed using the ABSMAD[35] program. Crystal data and structure solution and refinement parameters for compounds **1**, **3** and **6** are collected in Table 8.

Structure determination and refinement. The structures were solved by heavy-atom methods (SHELXS 86)[36] and subjected to full-matrix least-squares refinement based on F_o^2 (SHELXL 93[37]). Non hydrogen atoms were refined anisotropically with all hydrogens included in idealised positions, having isotropic thermal parameters riding on the value of their parent atoms. An absorption correction (DIFABS[38]) was applied to all three structures. The weighting scheme used was $w = 1/[\sigma^2(F_o^2)]$. Diagrams were drawn with SNOOPI.[39] Sources of scattering factor data are given in ref. 38.

Complete atomic coordinates, thermal parameters and bond lengths and angles have been deposited at the Cambridge Crystallographic Data Centre. See Instructions for Authors, *J. Chem. Soc., Dalton Trans.*, 1996, Issue 1.

Acknowledgements

We thank the EPSRC and BP Chemicals Ltd. for a CASE studentship (for S. J. C.), and to the EPSRC for support to the crystallography unit.

References

1 T. B. Rauchfuss and J. C. Jeffrey, *Inorg. Chem.*, 1979, **18**, 2658.
2 T. B. Rauchfuss, F. D. Patino and D. M. Roundhill, *Inorg. Chem.*, 1975, **14**, 652.
3 E. Lindner and A. Bader, *Coord. Chem. Rev.*, 1991, **108**, 27 and refs. therein.
4 P. Braunstein, D. G. Kelly, Y. Dusausoy, D. Bayeul, M. Lanfranchi and A. Tiripicchio, *Inorg. Chem.*, 1994, **33**, 233.
5 N. W. Alcock, A. W. G. Platt and P. Pringle, *J. Chem. Soc., Dalton Trans.*, 1987, 2273.
6 B. Demmerseman, C. Renouard, R. Le Lagadec, M. Gonzalez, P. Crochet and P. H. Dixneuf, *J. Organomet. Chem.*, 1994, **471**, 229.
7 See, for example, K. R. Dunbar and J.-S. Sun, *J. Chem. Soc., Chem. Commun.*, 1994, 2387; K. R. Dunbar, S. C. Haefner and C. Bender, *J. Am. Chem. Soc.*, 1991, **113**, 9540; A. Varshney, M. L. Webster and G. M. Gray, *Inorg. Chem.*, 1992, **31**, 2580; A. M. Allgeier, E. T. Singewald, C. A. Mirkin and C. L. Stern, *Organometallics*, 1994, **13**, 2928; M. Schulz and H. Werner, *Organometallics*, 1992, **11**, 2790; E. Lindner, M. Haustein, H. A. Mayer, K. Gierling, R. Fawzi and

M. Steimann, *Organometallics*, 1995, **14**, 2246; E. Lindner, R. Schreiber, M. Kemmler, H. A. Mayer, R. Fawzi and M. Steimann, *Z. Anorg. Allg. Chem.*, 1993, **619**, 202.
8 (*a*) P. Braunstein, S. C. Cea, A. DeCian and J. Fischer, *Inorg. Chem.*, 1992, **31**, 4203; (*b*) K. R. Dunbar, S. C. Haefner and A. Quillevéré, *Polyhedron*, 1990, **9**, 1695; (*c*) E. Lindner, M. Geprägs, R. Fawzi and M. Steimann, *Chem. Ber.*, 1993, **126**, 889.
9 (*a*) S.-T. Liu, G.-J. Liu, C.-H. Yieh, M.-C. Cheng and S.-M. Peng, *J. Organomet. Chem.*, 1990, **387**, 85; (*b*) T.-Y. Hsieh, M.-C. Cheng, S.-M. Peng and S.-T. Liu, *J. Chem. Soc., Dalton Trans.*, 1994, 3499; (*c*) M. R. Mason, Y. Su, R. A. Jacobson and J. G. Verkade, *Organometallics*, 1991, **10**, 2335; (*d*) T. C. Blagborough, R. Davis and P. Ivison, *J. Organomet. Chem.*, 1994, **467**, 85.
10 (*a*) K. R. Dunbar, S. C. Haefner and D. J. Burzynski, *Organometallics*, 1990, **9**, 1347; (*b*) K. R. Dunbar, J.-S. Sun, S. C. Haefner and J. H. Matonic, *Organometallics*, 1994, **13**, 2713; (*c*) A. Varshney and G. M. Gray, *Inorg. Chem.*, 1991, **30**, 1748; (*d*) M. R. Mason and J. G. Verkade, *J. Am. Chem. Soc.*, 1991, **113**, 6309; (*e*) M. R. Mason and J. G. Verkade, *Organometallics*, 1992, **11**, 1514.
11 P. B. Hitchcock, M. F. Lappert and I. A. MacKinnon, *J. Chem. Soc., Chem. Commun.*, 1993, 1015.
12 L. Miquel, M. Basso-Bert, R. Choukroun, R. Madhouni, B. Eichhorn, M. Sanchez, M.-R. Mazières and J. Jand, *J. Organomet. Chem.*, 1995, **490**, 21.
13 C. Masters, *Homogeneous Transition-metal Catalysis—a Gentle Art*, Chapman and Hall, London and New York, 1981.
14 H. B. Kagan and O. Riant, *Chem. Rev.*, 1992, **92**, 1007.
15 T. K. Hollis, N. P. Robinson and B. Bosnich, *J. Am. Chem. Soc.*, 1992, **114**, 5464; W. Odenkirk and B. Bosnich, *J. Chem. Soc., Chem. Commun.*, 1995, 1181.
16 S. Collins, B. E. Koene, R. Ramachandran and N. J. Taylor, *Organometallics*, 1991, **10**, 2092.
17 J. W. Falber and Y. Ma, *J. Am. Chem. Soc.*, 1991, **113**, 1579.
18 P. V. Bonnesen, C. L. Puckett, R. V. Honeycheck and W. H. Hersh, *J. Am. Chem. Soc.*, 1989, **111**, 6070.
19 S. J. Chadwell, S. J. Coles, P. G. Edwards, M. B. Hursthouse and Ahmed Imran, *Polyhedron*, 1995, **14**, 1057.
20 S. J. Chadwell, S. J. Coles, P. G. Edwards and M. B. Hursthouse, *J. Chem. Soc., Dalton Trans.*, 1995, 3551.
21 E. Lindner, Q. Wang, H. A. Mayer, R. Fawzi and M. Steimann, *Organometallics*, 1993, **12**, 1865.
22 D. L. Hughes, G. J. Leigh and D. C. Walker, *J. Organomet. Chem.*, 1988, **355**, 113; J. A. Albanese, D. L. Staley, A. L. Rheingold and J. L. Burmeister, *Inorg. Chem.*, 1990, **29**, 2209.
23 A. R. H. Al-Soudani, A. S. Batsanov, P. G. Edwards and J. A. K. Howard, *J. Chem. Soc., Dalton Trans.*, 1994, 987.
24 T. A. Magee, C. N. Matthews, T. S. Wang and J. H. Wotiz, *J. Am. Chem. Soc.*, 1961, **83**, 3200.
25 J. G. Verkade, *Coord. Chem. Rev.*, 1971, **9**, 1.
26 P. E. Garrou, *Chem. Rev.*, 1981, **81**, 229.
27 S. P. Gejji, K. Hermansson and J. Lindgren, *J. Phys. Chem.*, 1993, **97**, 3712.
28 G. A. Lawrence, *Chem. Rev.*, 1986, **86**, 17.
29 J. S. Haynes, S. J. Rettig, J. R. Sams, R. C. Thompson and J. Trotter, *Can. J. Chem.*, 1986, **64**, 429; V. Zanotti, S. Bordoni, L. Carlucci, V. G. Albano and D. Braga, *J. Chem. Soc., Dalton Trans.*, 1992, 1105.
30 M. Di Vaira, S. Midollini and L. Sacconi, *Inorg. Chem.*, 1981, **20**, 3430.
31 D. P. Tate, W. R. Knipple and J. M. Augl, *Inorg. Chem.*, 1962, **1**, 433.
32 R. J. Angelici, *J. Chem. Educ.*, 1968, **45**, 119.
33 S. R. Drake, M. B. Hursthouse, K. M. A. Malik and S. A. S. Miller, *Inorg. Chem.*, 1993, **32**, 4653.
34 J. W. Pflugrath and A. Messerschmidt. MADNES, version 11 September 1989, Delft Instruments, Delft, 1989.
35 ABSMAD, Program for FAST data processing, A. I. Karaulov, University of Wales, Cardiff, 1992.
36 G. M. Sheldrick, *Acta Crystallogr., Sect. A*, 1990, **46**, 467.
37 G. M. Sheldrick, University of Göttingen, 1993.
38 N. P. C. Walker and D. Stuart, *Acta Crystallogr., Sect. A*, 1983, **39**, 158; adapted for FAST geometry by A. I. Karaulov, University of Wales, Cardiff, 1991.
39 K. Davies and K. C. Prout, University of Oxford, 1993.

Received 6th *October* 1995; *Paper* 5/06597F